Polymorphism and Chain Conformations in the Crystalline Forms of Syndiotactic Poly(1-butene)

Claudio De Rosa,* Vincenzo Venditto, Gaetano Guerra, Beniamino Pirozzi, and Paolo Corradini

Dipartimento di Chimica, Università di Napoli Federico II, via Mezzocannone 4, 80134 Napoli, Italy

Received January 2, 1991; Revised Manuscript Received April 23, 1991

ABSTRACT: A preliminary structural characterization of syndiotactic poly(1-butene) (s-PB) is presented. X-ray diffraction analyses on powder and fiber samples show that s-PB can crystallize in two different crystalline forms, named form I and form II. Helical symmetries s(2/1)2 and s(5/3)2 with repetitions of 7.73 and 20.0 Å have been found for the chains in form I and form II, respectively. Different conformations of the lateral groups of the chains for the two crystalline forms are suggested on the basis of conformational energy calculations as well as of comparisons between the X-ray diffraction patterns and the calculated Fourier transforms for isolated model chains.

Introduction

Isospecific and syndiospecific polymerizations of 1-alkenes in the presence of homogeneous catalysts based on the group 4A metallocene/methylalumoxane systems have been recently reported.[1-5] In particular, two different kinds of syndiospecific catalytic systems have been discovered which work for styrene and substituted styrene[3,4] or for propene.[5] At variance with the old syndiospecific catalytic systems for propene polymerization (vanadium based and operating at low temperatures[6]), this new syndiospecific system for propene polymerization[5] is also able to produce highly syndiotactic polymers of other 1-alkenes.[7]

In this paper a preliminary characterization of the so-obtained highly syndiotactic poly(1-butene) (s-PB) is presented.

X-ray diffraction analyses on powder and fiber samples are reported which show that s-PB can crystallize in two different crystalline forms.

Possible conformations of the chains in both crystalline forms are suggested on the basis of conformational energy calculations as well as of comparison between the X-ray diffraction patterns and the calculated Fourier transforms for isolated model chains.

Experimental Procedure and Method of Calculations

The s-PB was supplied by the Himont Italia. The amount of rrrr pentads is equal to 93%.

Oriented amorphous samples were obtained by drawing at nearly 0 °C compression-molded amorphous samples. Oriented crystalline samples were then obtained by slow crystallization at room temperature for several days.

Wide-angle X-ray diffraction patterns were obtained with nickel-filtered Cu Kα radiation. The diffraction patterns of nonoriented samples were obtained with an automatic Philips diffractometer, while those for oriented samples were obtained with photographic cylindrical and flat cameras.

The DSC scans were carried out in a Mettler TA3000 (DSC-30) calorimeter in a flowing nitrogen atmosphere at a heating rate of 10 °C/min.

The conformational energy maps have been calculated with the method described in ref 8. We only recall that the nonbonded terms have been calculated by taking into account the interactions between the atoms (separated by more than two bonds) inside the evidenced conformational repeating unit of Figure 4 and the interactions between these atoms and all the remaining atoms. The angle increments for the energy maps are 10° for the maps of Figure 5 and 5° for the map of Figure 7 and the curves of Figure 8.

All the reported energies are referred to a monomeric unit and correspond to one-half of the energy calculated with this procedure. The potential energy constants are those reported by Flory,[9] treating only the CH_3 groups as spherical domains.[10]

The square of the modulus ($|F(\xi,\varphi,\zeta)|^2$) of the Fourier transform was calculated for each model as a function of the cylindrical reciprocal lattice coordinates ξ and ζ for a fixed value of the third coordinate φ. The mean value of $|F(\xi,\varphi,\zeta)|^2$ with respect to φ, henceforth indicated $\langle|F(\xi,\zeta)|^2\rangle$, was obtained by averaging the results for 90 different fixed rotations of the models around an axis parallel to the chain axes. The calculated intensities were multiplied by a "thermal factor" of the kind $\exp(-{}^1/_2B\xi^2)\exp(-{}^1/_2B\zeta^2)$ using an isotropic parameter, $B = 8$ Å^2.

Results and Discussion

X-ray Diffraction Patterns. The crystallizations of s-PB is a very slow process. In fact, by cooling from the melt or by precipitation or casting from polymer solutions, amorphous samples are generally obtained.

Some crystallinity, however, develops in s-PB samples maintained at room temperature for several days. The X-ray diffraction pattern of a compression-molded sample after 2 weeks of crystallization at room temperature is shown in Figure 1. From this and similar patterns degrees of crystallinity up to 50–60% have been evaluated. The melting and the glass transition temperatures of this crystalline form are close to +50 and −18 °C, respectively, as shown by the DSC scan of Figure 2.

Semicrystalline s-PB oriented samples can be easily obtained by drawing of amorphous samples followed by slow crystallization processes at room temperature. For low draw ratio values, the reflections in the fiber patterns are characterized by diffraction angles and relative intensities (Table I) which well correspond to those of powder patterns like that of Figure 1.

For high draw ratio values (>100%), together with these reflections, new reflections appear in the fiber spectra (Table II), which are indicative of a second crystalline form.

The two crystalline forms, whose reflections are listed in Tables I and II, will be named thereafter forms I and II.

Form I shows the presence of two different layer lines, besides the equatorial layer line, whose ζ reciprocal coordinates are consistent with l indexes 1 and 2 for a repeating unit $c = 7.6 \pm 0.3$ Å. A more accurate value, c

0024-9297/91/2224-5645$02.50/0

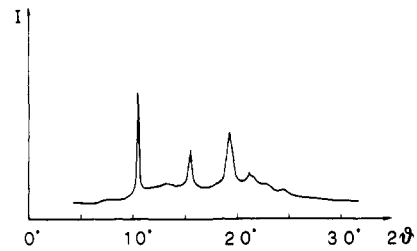

Figure 1. X-ray diffraction pattern of a compression-molded sample after 2 weeks of crystallization at room temperature.

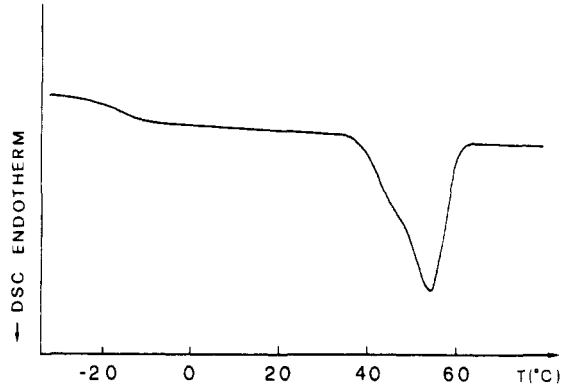

Figure 2. DSC scan of the sample of Figure 1.

Table I
Diffraction Angles 2θ, Bragg Distances *d*, and Reciprocal Coordinates ξ and ζ of the Reflections on the Layer Lines *l* in the X-ray Fiber Patterns of Form I

2θ, deg	*d*, Å	ξ, Å^{-1}	ζ, Å^{-1}	*l*	intensity[a]
10.5	8.42	0.119	0.0	0	s
15.55	5.72	0.175	0.0	0	m
21.5	4.13	0.242	0.0	0	w
19.5	4.56	0.175	0.133	1	s
24.4	3.65	0.240	0.133	1	w
23.0	3.87	0.0	0.258	2	s

[a] s = strong, m = medium, w = weak.

Table II
Diffraction Angles 2θ, Bragg Distances *d*, and Reciprocal Coordinates ξ and ζ of the Reflections on the Layer Lines *l* in the X-ray Fiber Patterns of Form II

2θ, deg	*d*, Å	ξ, Å^{-1}	ζ, Å^{-1}	*l*	intensity[a]
12.0	7.38	0.136	0.0	0	w
13.0	6.81	0.147	0.0	0	s
13.75	6.44	0.155	0.0	0	s
17.5	5.07	0.197	0.0	0	vw
22.75	3.91	0.256	0.0	0	vw
25.0	3.56	0.281	0.0	0	vw
20.8	4.27	0.229	0.0508	1	m
21.6	4.11	0.238	0.0508	1	m
22.2	4.0	0.228	0.101	2	vw
18.7	4.75	0.149	0.149	3	s
20.5	4.33	0.120	0.197	4	mw
22.4	3.97	0.157	0.197	4	mw
23.4	3.80	0.174	0.197	4	mw
23.0	3.87	0.0	0.250	5	s

[a] s = strong, m = medium, w = weak, mw = medium weak, vw = very weak.

= 7.73 ± 0.07 Å, has been obtained by tilted fiber spectra. These data are consistent with a helical symmetry of the kind s(2/1)2, in which the chain repetition occurs after 2 conformational repeating units[11] (4 monomeric units) and after 1 turn around the chain axis. This kind of symmetry has been also observed in polymorphic forms of syndiotactic polypropene (s-PP),[12] syndiotactic polystyrene (s-PS),[8,13,14] and syndiotactic poly(*p*-methylstyrene).[15]

Table III
Lowest Values of the Indexes of the Bessel Functions Contributing to the X-ray Intensity on the Layer Lines *l* for (5/1), (5/2), (5/3), and (5/4) Helices Compared to the Observed Intensities

l	(5/1)	(5/2)	(5/3)	(5/4)	intensity[a]
0	0	0	0	0	s
1	1	-2	2	-1	m
2	2	1	-1	-2	vw
3	-2	-1	1	2	s
4	-1	2	-2	1	mw
5	0	0	0	0	s

[a] s = strong, m = medium, w = weak, mw = medium weak, vw = very weak.

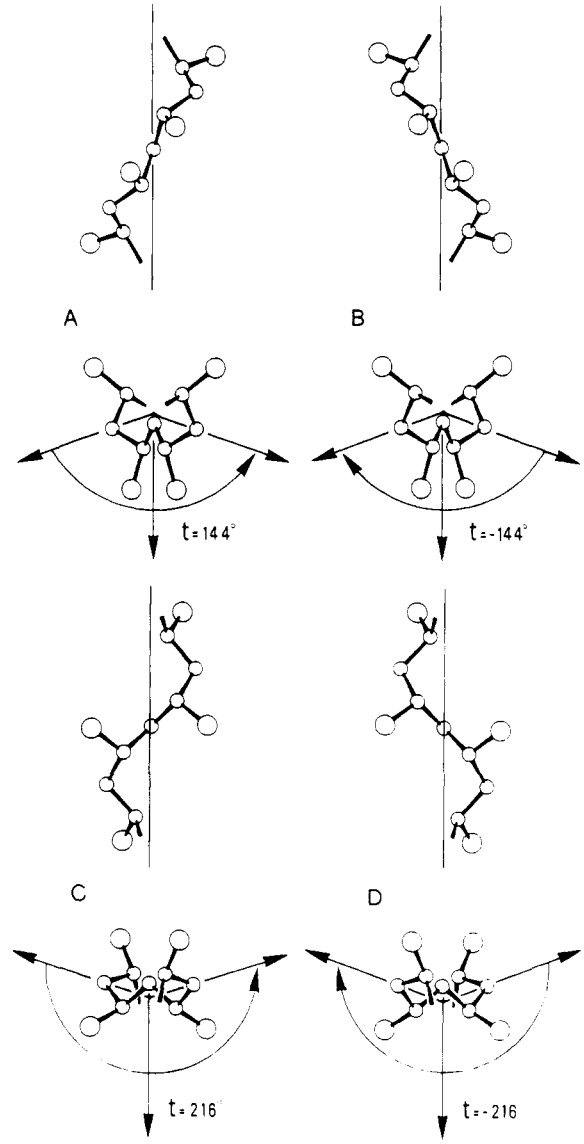

Figure 3. Side views and projections along the chain axis of the helices having the unit height observed for form II of s-PB (4.0 Å): (A) right-handed helix with a (5/2)2 symmetry (t = 144°); (B) left-handed helix with a (5/2)2 symmetry (t = -144°); (C) right-handed helix with a (5/3)2 symmetry (t = 216°); (D) left-handed helix with a (5/3)2 symmetry (t = -216°). In the projection along the chain axis the convention used to define the unit twist (t) is also shown (see text).

Form II shows the presence of five different layer lines, besides the equatorial layer line, whose ζ reciprocal coordinates are consistent with *l* indexes 1, 2, 3, 4, and 5 for a repeating unit c = 20.0 ± 0.3 Å. These data are consistent with a helical symmetry of the kind s(5/*N*)2, in which the chain repetition occurs after 5 conforma-

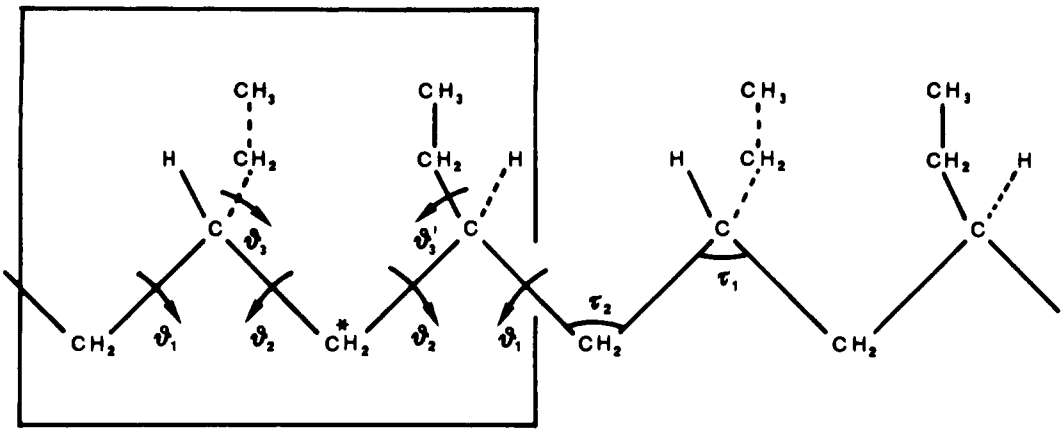

Figure 4. Portion of the chain of s-PB considered in the energy analysis. Both torsion angles, which characterize the conformations of the lateral groups in the conformational repeating units (θ_3, θ_3'), are defined with respect to the same CH_2 group (indicated by an asterisk). The binary axis, crossing the CH_2 groups of the main chain, for the s(M/N)2 symmetry imposes $\theta_3 = \theta_3'$.

tional repeating units (10 monomeric units) and after N turns of the main-chain atoms around the chain axis. A qualitative comparison between the average intensities on the layer lines of form II and the lowest values of the indexes of the Bessel functions contributing to them[16] is presented in Table III for the cases of N = 1, 2, 3, and 4. This qualitative comparison does not give sufficient elements to discard any of the possible s(5/N)2 helical conformations.

Geometrical Considerations Relative to the s(5/N)2 Helices. In conventional crystallographic symmetry, 5_2 and 5_3 (or 5_1 and 5_4) screw axes correspond to helices that are of opposite twist sense but otherwise equivalent.

Also s(5/2) and s(5/3) helices formed by macromolecular chains in several cases are equivalent but enantiomorphous. This is, for instance, observed for the case of helices containing all equivalent atoms on the helical backbone (one-atom helices).

In the present case, it is instead possible to define nonequivalent s(5/2)2 and s(5/3)2 (or s(5/1)2 and s(5/4)2) helices in analogy with previous literature reports,[17-19] as detailed in the following.

To show their nonequivalence, Figure 3 presents two different views of the (5/2) and (5/3) right- and left-handed helices having the same values of the unit height (4.0 Å). The figure also shows the convention we use for the definition of the unit twist ($t = 2\pi N/M$). Let us associate vectors every two binary axes, perpendicular to the chain axis and having their origin on the chain axis, in the direction which bisects the H–C–H bond angle; at the alternate binary axes let us associate vectors in the direction opposite to that which bisects the H–C–H bond angle (nonequivalent to that considered previously). Any set of three such vectors, succeeding each other along the chain axis, defines a right- or left-handed helix sense and the unit twist.

The pairs of enantiomorphous helices A,B and C,D are not equivalent. In particular, according to the present definition of t, A and B are (5/2) helices, right- and left-handed, respectively ($N = |t| \times 5/2\pi = 2$), while C and D are (5/3) helices, right- and left-handed, respectively ($N = |t| \times 5/2\pi = 3$).

Conformational Energy Calculations. Application of the equivalence principle[20] to successive constitutional units in a syndiotactic polymer leads to s(M/N)2 and tc (helical and glide plane) symmetries for the chain. The observed values of the chain axis allow us to discard the tc symmetry. Therefore conformational energy calculations have been performed by assuming a line repetition group s(M/N)2 for the polymer chain. As a consequence the sequence of the torsion angles in the main chain for which the calculations has been performed is of the kind ...θ_1, θ_1, θ_2, θ_2... (Figure 4).

Table IV
Bond Lengths and Bond Angles Used in the Conformational Energy Maps of s-PB

	Bond Lengths, Å		
C–C	1.53	C–H	1.10
	Bond Angles,[a] deg		
C″–C′–C″	111.0	C′–C″–H	108.9
C′–C″–C′	113.0	H–C″–H	108.0
C″–C′–H	107.9		

[a] C′ indicates a methine carbon atom; C″ indicates a methylene carbon atom.

It is also assumed that the binary axes crossing the methylene groups of the main chain, typical of the line repetition group s(M/N)2, relate also the atoms of the lateral groups. In order to attribute equal numerical values to the dihedral angles of the lateral groups, the definition for θ_3 reported in the caption of Figure 4 is assumed. The values of the geometrical parameters assumed in the present calculations are reported in Table IV. A conformational energy map for s-PB as a function of θ_1 and θ_2, scanned every 10° in θ_3 (minimum-energy values reported), is shown in Figure 5. Two equivalent absolute minima are located at $\theta_1 \approx G^+$, $\theta_2 \approx T$ and $\theta_1 \approx T$, $\theta_2 \approx G^-$, while the energy minimum corresponding to a trans-planar conformation has 3 kJ/mol higher energy.

The loci of the points corresponding to the (2/1) helical symmetry and to the value of the unit height observed for form I ($h = c/2 = 3.86$ Å) are shown in the map of Figure 6A, while the loci of points corresponding to the (5/N) helical symmetries and to the value of the unit height observed for form II ($h = c/5 = 4.0$ Å) are shown in the map of Figure 6B. The intersection points of the curves in Figure 6A,B indicate the θ_1,θ_2 pairs which correspond to the considered helical symmetries for the unit height values observed for forms I and II, respectively.

A detail of the energy map of Figure 5 (with θ_3 scanned every 5°) is reported in Figure 7, showing also the corresponding intersection points of Figure 6A,B. It is apparent that, for the observed values of the unit heights, two conformations, having (2/1) and (5/3) symmetries, are very close to the two separate regions in which the absolute conformational energy minimum of Figure 7 is split. On the contrary, the conformations with (5/1), (5/

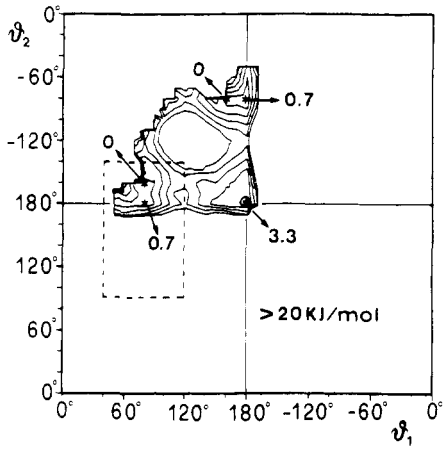

Figure 5. Map of the conformational energy of s-PB as a function of θ_1 and θ_2, scanned every 10° in θ_3, in the s(M/N)2 line repetition group for $\tau_1 = 111°$, $\tau_2 = 113°$. The curves are reported at intervals of 4 kJ/mol of monomeric units with respect to the absolute minimum of the map assumed as zero. A dashed rectangle indicates the detail which is enlarged in Figure 7.

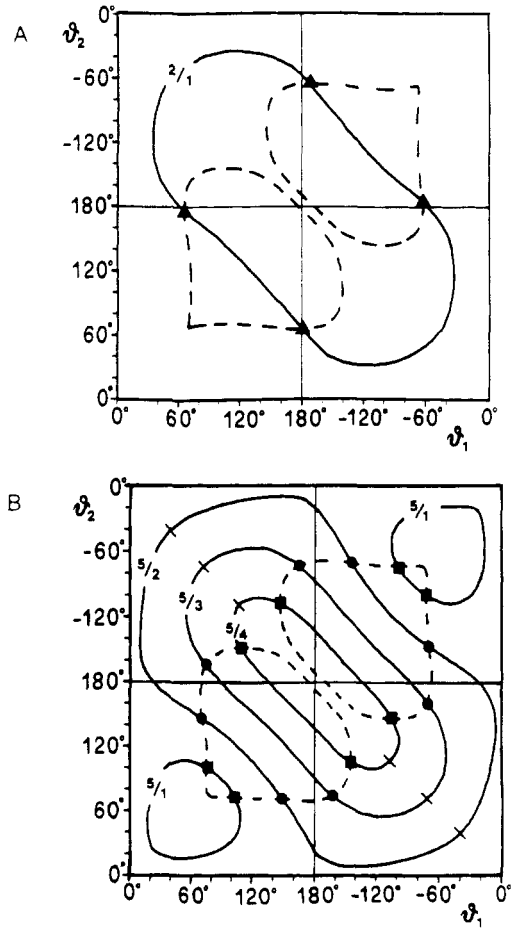

Figure 6. (A) Map as a function of θ_1 and θ_2 of the loci of points for which the helical symmetry is s(2/1)2 (continuous lines) and h = 3.86 Å (dashed lines). The intersection points are indicated by triangles. (B) Map as a function of θ_1 and θ_2 of the loci of points for which the helical symmetry is s(5/N)2 (continuous lines) and h = 4.0 Å (dashed lines). The intersection points for the s(5/4)2 and s(5/1)2 symmetries are indicated by squares while the intersection points for the s(5/3)2 and s(5/2)2 symmetries are indicated by circles.

2), and (5/4) symmetries do not correspond to energy minima, and much higher energies are involved (>16 kJ/mol).

This strongly suggests that the chain conformation in crystalline form II of s-PB has a (5/3) symmetry.

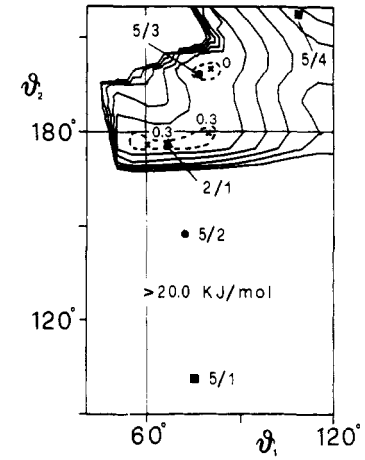

Figure 7. A detail of the energy map of Figure 5. The intersection points of Figure 6 are also shown, using the same symbols of Figure 6. The isoenergetic curves correspond to 1, 4, 8, 12, 16, and 20 kJ/mol of monomeric units. The values of the energies corresponding to the minima (×) are also indicated.

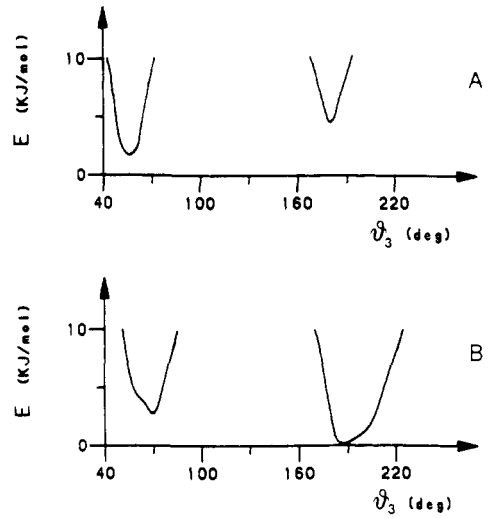

Figure 8. Curves of the conformational energy as a function of θ_3 for (A) model chain with s(2/1)2 symmetry with θ_1 = 66° and θ_2 = 176° and (B) model chain with s(5/3)2 symmetry with θ_1 = 74° and θ_2 = 196.5°.

We recall that a chain conformation with (5/2) helical symmetry has been instead found for syndiotactic poly(α-methylvinyl methyl ether)[17] and has been also suggested for syndiotactic poly(methyl methacrylate).[21]

According to the present geometrical and energy analysis, the values of the dihedral angles along the main chain of the s-PB for the (2/1) helix of form I and for the (5/3) helix of form II can be assumed close to the values of the intersection points of Figure 7 (θ_1 = 66°, θ_2 = 176° and θ_1 = 74°, θ_2 = 196.5°, respectively). For these two fixed pairs of (θ_1,θ_2) values assumed for form I and form II, conformational energy curves as a function of the dihedral angle θ_3 (which characterizes the conformations of the lateral ethyl groups) are reported in Figure 8A and 8B, respectively.

It is apparent that two conformations, in particular those presenting $\theta_3 \approx 60°$ and $\theta_3 \approx 180°$, correspond to energy-minimum situations for both models of form I and form II.

However, according to the present energy calculations, the conformation with $\theta_3 \approx 60°$ is favored for s(2/1)2 (model chain of form I) (Figure 8A), while the conformation with $\theta_3 \approx 180°$ is favored for s(5/3)2 (model chain of form II) (Figure 8B).

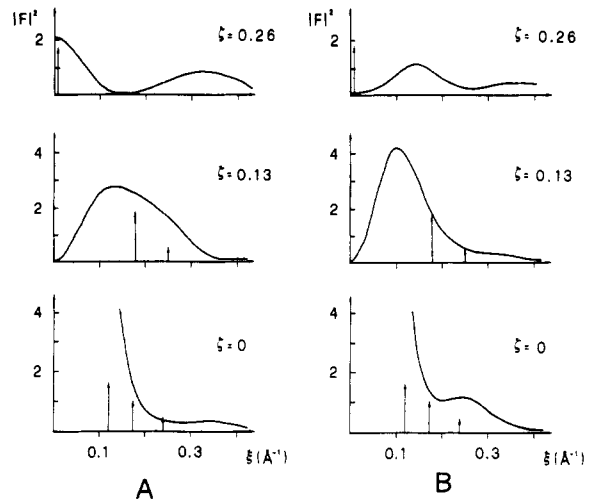

Figure 9. Fourier transforms, calculated on the layer lines at the indicated values of the reciprocal coordinate ζ (Å^{-1}), for the minimum-energy models of s-PB with s(2/1)2 helical symmetry for which (A) $\theta_3 = 60°$ and (B) $\theta_3 = 180°$. A qualitative comparison with the observed X-ray intensities for form I is also reported.

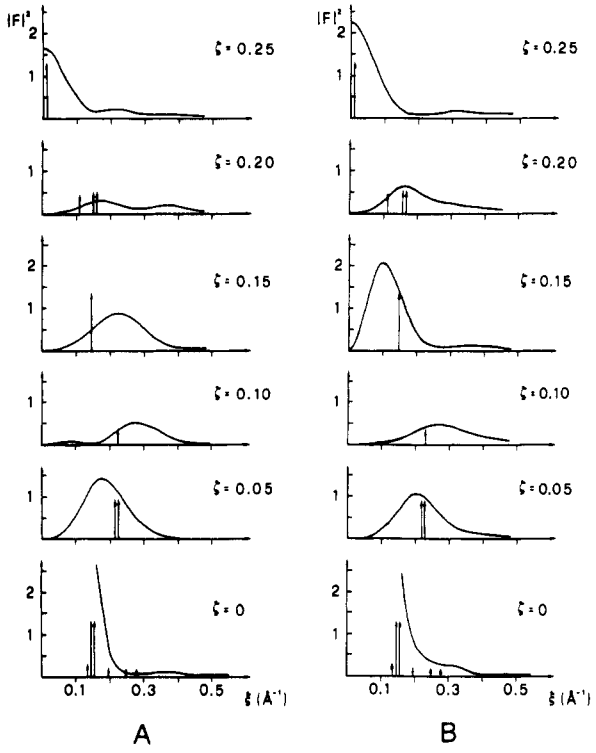

Figure 10. Fourier transforms, calculated on the layer lines at the indicated values of the reciprocal coordinate ζ (Å^{-1}), for the minimum-energy models of s-PB with s(5/3)2 helical symmetry for which (A) $\theta_3 = 60°$ and (B) $\theta_3 = 180°$. A qualitative comparison with the observed X-ray intensities for form II is also reported.

Fourier Transform Calculations for Isolated Model Chains. Fourier transform calculations for isolated model chains of s-PB with s(2/1)2 helical symmetry and $h = 3.86$ Å or s(5/3)2 symmetry and $h = 4.0$ Å are shown in Figures 9 and 10, respectively. For both helical symmetries, both conformations of the lateral groups with $\theta_3 \approx 60°$ and $\theta_3 \approx 180°$ are considered, and the corresponding Fourier transforms are reported in parts A and B, respectively, of Figures 9 and 10. A qualitative comparison with the observed X-ray intensities of form I and form II is also presented in Figures 9 and 10, respectively.

For the case of form I, only the model with $\theta_3 \approx 60°$ gives a good qualitative agreement between calculated and experimental X-ray diffraction patterns. In fact, the meridional reflection on the second layer line corresponds to a calculated minimum of the Fourier transform for the model with $\theta_3 \approx 180°$ (Figure 9B).

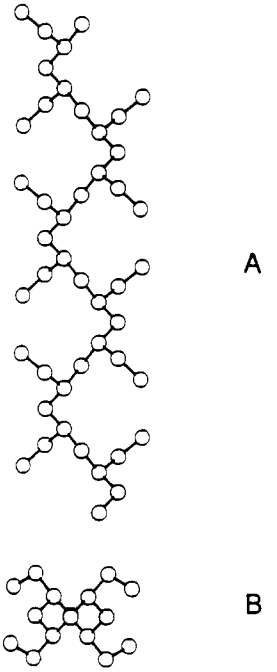

Figure 11. Side view (A) and a projection along the chain axis (B) of the model suggested for the chain conformation of form I of s-PB.

This result of the Fourier transform analysis compares well with the energy analysis of the previous section (Figure 8A), which indicates the conformation with $\theta_3 \approx 60°$ is more favored for the s(2/1)2 helix of form I. The projection along the chain axis and a side view of the model suggested for the chain conformation in form I of s-PB are sketched in Figure 11.

For the case of models with an s(5/3)2 helical symmetry, the difference between the calculated Fourier transforms for different conformations of the lateral groups are less pronounced (cf. Figure 10A,B). However, a difference in the position and the height of the calculated intensity maxima on the third layer line is present. In fact, for $\theta_3 \approx 60°$ this maximum is located at $\xi = 0.22$ Å^{-1} and is weaker than the maximum on the first layer line, while for $\theta_3 \approx 180°$ it is located $\xi = 0.10$ Å^{-1} and is stronger than the maximum on the first layer line. Since the experimental pattern of form II presents on the third layer line a strong reflection at $\xi = 0.14$ Å^{-1}, this analysis seems to suggest as more suitable for the s(5/3)2 helix the conformation with $\theta_3 \approx 180°$.

Again the suggestion of the Fourier analysis compares well with the energy analysis (Figure 8B), which indicates the conformation with $\theta_3 \approx 180°$ is more favored for the s(5/3)2 helix of form II.

The projection along the chain axis and a side view of the model suggested for the chain conformation in form II of s-PB are sketched in Figure 12.

Conclusions

Syndiotactic poly(1-butene) (s-PB) crystallizes in two different crystalline forms. Both crystalline forms of s-PB are characterized by helical conformations of the chains of the kind $\approx TTG^+G^+$ (right-handed) or $\approx G^-G^-TT$ (left-handed). A helical symmetry of the kind s(2/1)2 with a chain repetition $c = 7.73$ Å has been found for the chains in form I, while a helical symmetry of the kind s(5/3)2

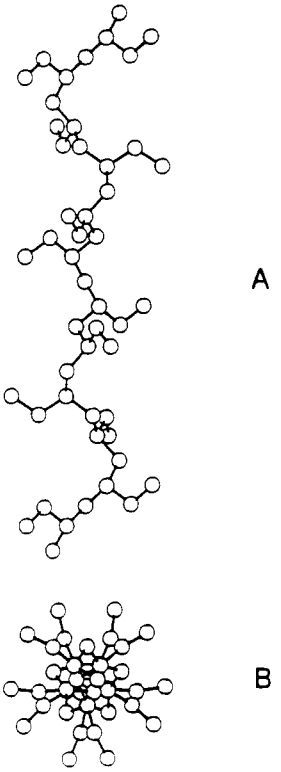

Figure 12. Side view (A) and a projection along the chain axis (B) of the model suggested for the chain conformation of form II of s-PB.

with a chain repetition c = 20.0 Å characterizes the conformation of the chains in form II.

Different conformations of the lateral group of the chains in the two crystalline forms are suggested on the basis of conformational energy calculations as well as of comparisons between the X-ray diffraction patterns and the calculated Fourier transforms for isolated model chains.

In particular, the two conformations, presenting $\theta_3 \approx 60°$ and $\theta_3 \approx 180°$, correspond to energy-minimum situations for both models of form I and form II. However, the conformation with $\theta_3 \approx 60°$ is energetically favored for the s(2/1)2 helix (model chain of form I), while the conformation with $\theta_3 \approx 180°$ is favored for the s(5/3)2 helix (model chain of form II). On the other hand, the comparisons between the X-ray diffraction patterns and the calculated Fourier transforms for isolated chains also suggest that the conformation with $\theta_3 \approx 60°$ is possibly more suitable for the s(2/1)2 helix of form I, while that with $\theta_3 \approx 180°$ is possibly more suitable for the s(5/3)2 helix of form II.

Acknowledgment. We thank Dr. E. Albizzati and Dr. L. Resconi of the Himont Italia for useful discussions. This work was supported by the Ministero dell'Università e della Ricerca Scientifica e Tecnologica and by the Progetto Finalizzato Chimica Fine e Secondaria of the CNR.

References and Notes

(1) Ewen, J. A. *J. Am. Chem. Soc.* **1984**, *106*, 6355.
(2) Kaminsky, W.; Kuple, K.; Brintzinger, H. H.; Wild, F. R. W. P. *Angew. Chem., Int. Ed. Engl.* **1985**, *24*, 507.
(3) Ishihara, N.; Seimiya, T.; Kuramoto, M.; Koi, M. *Macromolecules* **1986**, *19*, 2464.
(4) Zambelli, A.; Longo, P.; Pellecchia, C.; Grassi, A. *Macromolecules* **1987**, *20*, 2035.
(5) Ewen, J. A.; Jones, R. L.; Razavi, A.; Ferrara, J. D. *J. Am. Chem. Soc.* **1988**, *110*, 6255.
(6) Natta, G.; Pasquon, I.; Zambelli, A. *J. Am. Chem. Soc.* **1962**, *84*, 1488.
(7) Albizzati, E.; Zambelli, A.; Resconi, L. Eur. Pat. Appl., 387609, (Himont Inc.), 1990.
(8) Corradini, P.; Napolitano, R.; Pirozzi, B. *Eur. Polym. J.* **1990**, *26*, 157.
(9) Yoon, D. Y.; Sundararajan, P. R.; Flory, P. J. *Macromolecules* **1975**, *8*, 765.
(10) Sundararajan, P. R.; Flory, P. J. *J. Am. Chem. Soc.* **1974**, *96*, 5025.
(11) IUPAC Commission on Macromolecular Nomenclature. *Pure Appl. Chem.* **1981**, *53*, 733.
(12) Corradini, P.; Natta, G.; Ganis, P.; Temussi, P. A. *J. Polym. Sci., Part C* **1967**, *16*, 2477.
(13) Immirzi, A.; De Candia, F.; Iannelli, P.; Vittoria, V.; Zambelli, A. *Makromol. Chem., Rapid Commun.* **1988**, *9*, 761.
(14) Guerra, G.; Vitagliano, V. M.; De Rosa, C.; Petraccone, V.; Corradini, P. *Macromolecules* **1990**, *23*, 1539.
(15) Iuliano, M.; Guerra, G.; Petraccone, V.; Corradini, P.; Pellecchia, C. *New Polym. Mater.*, in press.
(16) Cochran, W.; Crick, F. H. C.; Vand, V. *Acta Crystallogr.* **1952**, *5*, 581.
(17) Chen, V. Y.; Allegra, G.; Corradini, P.; Goodman, M. *Macromolecules* **1970**, *3*, 274.
(18) Liguori, A. M. *Acta Crystallogr.* **1955**, *8*, 345.
(19) Uchida, T.; Tadokoro, H. *J. Polym. Sci.* **1967**, *5*, 63.
(20) Corradini, P. In *The Stereochemistry of Macromolecules*; Ketley, A. D., Ed.; Marcel Dekker Inc.: New York, 1968; Vol. 3.
(21) Brandrup, J.; Immergut, E. H. *Polymer Handbook*; J. Wiley & Sons, Inc.: New York, 1989; Chapter VI, p 19.

Registry No. *s*-PB, 131724-38-4.